J Physiol 591.23 (2013) pp 5843–5849

TECHNIQUES FOR PHYSIOLOGY

Optical determination of intracellular water in apoptotic cells

Michael A. Model[1] and Ethan Schonbrun[2]

[1] *Department of Biological Sciences, Kent State University, Kent, OH, USA*
[2] *Rowland Institute at Harvard, Harvard University, Cambridge, MA, USA*

Key points

- Determination of intracellular water can be achieved by a combination of brightfield and transmission-through-dye imaging, all realized on a standard transmission microscope.
- The method permits sensitive detection of water loss in cells exposed to apoptotic agents.
- Cell water measurements are not affected by separation of apoptotic bodies and can be applied to samples where measurements of cell volume alone would be insufficient.

Abstract Intracellular water plays a critical role in apoptotic and necrotic cell death. We describe a method for quantifying cell water by application of two previously described variants of transmission microscopy. By taking two axially displaced brightfield images, the phase shift of the transmitted wave was computed using the transport-of-intensity equation. At the same time, cell thickness was determined by transmission through an externally applied dye ('transmission-through-dye' microscopy); switching between these two imaging modalities was accomplished by simply changing the illumination wavelength. The sets of data thus obtained allow computation of the refractive index and cell water content within individual cells. The method was illustrated using cells treated with apoptotic agents staurosporine and actinomycin D and with necrosis inducer ionomycin. Water imaging allows discrimination between apoptotic volume decrease due to dehydration from that due to detachment of apoptotic bodies and can be used on samples where cell volume determination alone would be difficult or insufficient.

(Received 2 August 2013; accepted after revision 7 October 2013; first published online 14 October 2013)

Corresponding author M. A. Model: 1275 University Esplanade, Department of Biological Sciences, Kent State University, Kent, OH 44242, USA. Email: mmodel@kent.edu

Abbreviations AB9, Acid Blue 9; ActD, actinomycin D; TIE, transport-of-intensity equation; TTD, transmission-through-dye.

Introduction

Cell death is accompanied by dramatic changes in intracellular water. Necrotic cells absorb water, increase in size and eventually burst. By contrast, apoptosis is characterized by the loss of water; the resulting shrinkage was even used to initially recognize apoptosis as a distinct type of cell death (Kerr *et al.* 1972) and since then has been confirmed as an essential apoptotic feature. Much research effort has been directed at understanding the mechanisms and the role of apoptotic water loss (Gómez-Angelats & Cidlowski, 2002; Orlov *et al.* 2013).

Volume changes in apoptotic cells have been studied mostly by electronic sizing or by flow cytometry of cell suspensions, but also by microscopic methods, such as atomic force (Hessler *et al.* 2005), confocal scanning (Chacon *et al.* 1994), dual-image surface reconstruction (Platonova *et al.* 2011) or transmission-through-dye imaging (Kasim *et al.* 2013). However, the use of cell volume as a marker of intracellular water has its limitations. For example, apoptotic cells decrease in size not only through the loss of water but also by dissociation of apoptotic bodies. To our knowledge, reliable quantification of apoptotic bodies has not been developed, and even their mere detection under the microscope can be problematic if the detached particles come off the substrate. Therefore, a better alternative would be to measure cell water directly. The optical parameter most

© 2013 The Authors. The Journal of Physiology © 2013 The Physiological Society

DOI: 10.1113/jphysiol.2013.263228

The Journal of Physiology

closely related to intracellular water content is the average refractive index of the cell n; it is slightly higher than the refractive index of water, and therefore changes in cell hydration produce changes in the refractive index. A common approach to refractive index measurement combines determination of the phase ($\Delta\varphi$) of optical waves passing through an object with an independent measurement of the object thickness h (Curl *et al.* 2005; Tychinsky & Tikhonov, 2010). Since

$$\Delta\varphi = \frac{2\pi}{\lambda} h(n - n_{\text{medium}}) \tag{1}$$

the knowledge of $\Delta\varphi$, h and the wavelength λ allows determination of n.

In this report we examine the utility of this approach for cell death studies. We use perhaps the technically simplest of the quantitative phase techniques based on just two brightfield images. These images are collected at different distances to the object and are analysed by means of the transport-of-intensity equation (TIE), which relates $\Delta\varphi$ to the gradient of intensity $\frac{\partial I}{\partial z}$ along the optical axis (Barty *et al.* 1998):

$$\nabla_{xy}[I_0(x, y)\nabla_{xy}\varphi(x, y)] = -k\frac{\partial I(x, y, z)}{\partial z}\bigg|_{z=0} \tag{2}$$

In the above equation k denotes the wavenumber, I_0 the in-focus intensity and ∇_{xy} the gradient within the xy object plane. For the purpose of computation, the gradient is approximated by the difference of two images taken near the best focus.

To find h we use the transmission-through-dye (TTD) method, which has a similar advantage of requiring nothing more than a standard transmission microscope. In the TTD method, a non-penetrating dye with a strong absorption in the visible range is added to the sample, so that transmitted intensity quantitatively reflects cell thickness and volume (Antón *et al.* 2012; Model, 2012; Schonbrun *et al.* 2013).

Methods

Cell death experiments

Cells from the HeLa cell line were cultured in 5% CO_2 on loose coverslips in RPMI-1640 medium (Sigma-Aldrich, St Louis, MO, USA) supplemented with 10% fetal bovine serum (Atlanta Biologicals, Lawrenceville, GA, USA) and 1% antibiotic–antimycotic solution (Fisher Scientific, Suwanee, GA, USA) containing 10,000 IU ml^{-1} penicillin, 10 mg ml^{-1} streptomycin and 25 μg ml^{-1} amphotericin B; cells from the Madin–Darby bovine kidney (MDBK) cell line were cultured in DMEM medium with the same additives. Apoptosis was induced by 0.4 μM actinomycin D (ActD) or by 5 μM staurosporine (both from Sigma-Aldrich) for 14 and 3 h, respectively. Approximately 15 min before microscopic observation, the medium was replaced with one containing additionally 7 mg ml^{-1} Acid Blue 9 (AB9; TCI America, Portland, OR, USA). Because TTD imaging requires placing the sample in a shallow gap, the coverslips with cells were mounted in the same medium on slides over small spots of silicone grease that acted as a spacer. High concentrations of the calcium ionophore ionomycin caused rapid necrotic changes in HeLa cells, and therefore RPMI with AB9 and 10 μM ionomycin (Santa Cruz Biotechnology, Santa Cruz, CA, USA) was applied directly under the coverslip immobilized on a slide.

Anisosmotic treatment

HeLa cells were grown in coverslip-bottom dishes and equilibrated in AB9-containing Leibovitz L15 medium (Sigma-Aldrich). To create a thin layer of absorbing liquid directly in dishes, a conical attachment for the condenser with a watertight horizontal window was built; it was slowly lowered into the dish by turning its lower part on a fine-pitch thread to achieve the required thin gap over the cells (see Supplemental Fig. S1 available online).

Keeping an open dish on a microscope stage allows for fast and efficient replacement of the medium. The hypertonic medium contained the same components plus 0.15 M NaCl, and for the hypotonic medium we used 50% L15; AB9 was present in all solutions at the same concentration. The osmolality of these solutions was measured on a vapour pressure osmometer Vapro 5520 (Wescor, Logan, UT, USA) and was found to be 330 mosmol kg^{-1} (L15), 170 mosmol kg^{-1} (50% L15) and 620 mosmol kg^{-1} (L15 with NaCl).

Image acquisition

An Olympus IX70 microscope with a 20/0.7 PlanApo objective and an NA 0.55 condenser were used for all experiments. TTD images were acquired through a 630/10 bandpass filter (Omega Optical, Brattleboro, VT, USA) and brightfield images through a 485/10 filter (Omega Optical), where the absorption of AB9 is negligible. The vertical movement of the objective was achieved by a ProScan II stage controller (Prior Scientific, Rockland, MA, USA). Microscope hardware was controlled with Slidebook (Intelligent Imaging Innovations, Denver, CO, USA) and the images were captured with a SensiCam QE camera (Cooke, Romulus, MI, USA).

Image analysis

Cell volume was found from logarithmic images

$$h = \frac{\ln I}{\alpha} \tag{3}$$

© 2013 The Authors. The Journal of Physiology © 2013 The Physiological Society

where the difference between the local grey level and the background represents cell height h; α stands for the absorption coefficient of the medium and was measured to be $\alpha_{630} \approx 0.165\ \mu m^{-1}$ for 7 mg ml^{-1} AB9 by the lens immersion method (Model *et al.* 2008).

The phase map was computed from two brightfield images, one of which was chosen close to the best-focus plane and the other shifted into the sample by 1 μm. The calculations were performed using MatLab 7 (MathWorks, Natick, MA, USA) as reported previously (Gorthi & Schonbrun, 2012); the necessary files can be found in the Supplemental material available online. Phase images generated by TIE often suffer from non-uniform background, which partly arises from slight intensity fluctuations between the two input images. This problem can sometimes be alleviated either by high-pass digital filtering of the final image or by performing $\Delta\varphi$ computation on two flat images whose intensities are made equal to the average intensities of the original images; the result of the latter is an intensity profile that resembles the background in the actual phase image, thus enabling correction. To ensure correct estimation of the local background (which was usually determined within a 1 μm-wide band drawn around the cell), the phase integrated over the cell area was computed on both filtered and raw images, and the results were counted only if both numbers were within 5%. The refractive index difference between the cell and the medium was found from the total phase ($\Sigma\Delta\varphi$) integrated over the cell area and the cell volume V as

$$\Delta n = n - n_{\text{medium}} = \frac{\lambda}{2\pi V}\sum \Delta\varphi \qquad (4)$$

where $n_{\text{medium}} = 1.337$ (Curl *et al.* 2005; Lue *et al.* 2006; Gu *et al.* 2008). A set of images illustrating the process of refractive index measurement is shown in Fig. 1.

Conversion of the phase difference into cell water content

The parameter frequently used in quantitative studies of water balance is the volume fraction w occupied by

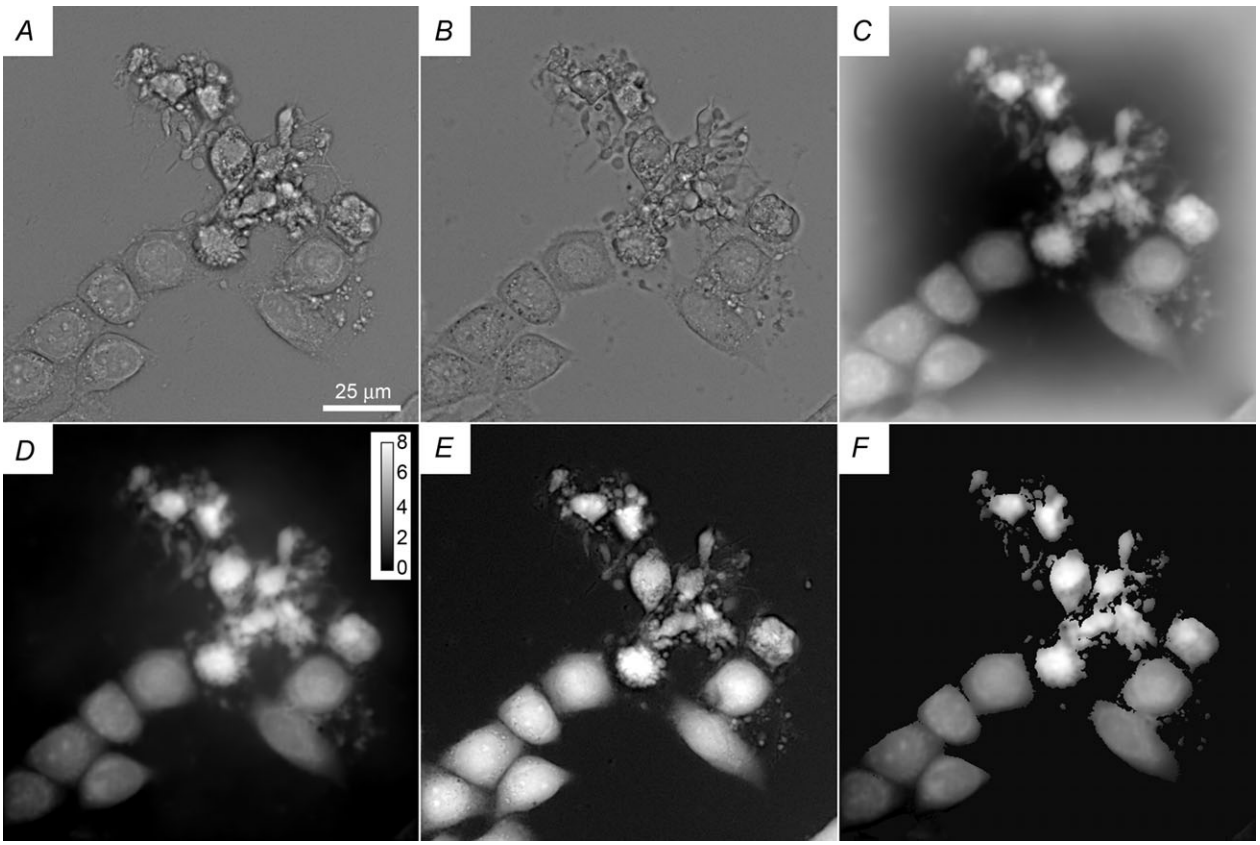

Figure 1. Example of image processing
A and *B*, two brightfield images of ActD-treated HeLa cells taken at a 1 μm vertical separation. *C*, phase image computed from images *A* and *B*. *D*, result of background correction on image *C* based on two flat images, as described in the text with a bar showing the scale in radians. *E*, TTD image representing cell thickness. *F*, a map of *n* obtained by dividing *D* by *E* and masking out the background areas; this image is only semi-quantitative because the background correction in *D* is not perfect.

© 2013 The Authors. The Journal of Physiology © 2013 The Physiological Society

intracellular water. Because protein accounts for most of the dry mass of a typical cell (Prescher & Bertozzi, 2005), we can approximately represent the total cell volume as a sum of the volumes occupied by protein and by water:

$$V = V_p + V_w = \frac{C_p}{d_p} V + wV \quad (5)$$

where C_p denotes the protein concentration and $d_p \approx 1.4\,\mathrm{g\,ml^{-1}}$ is the density of pure protein (Fischer *et al.* 2004). C_p can be found from the refractive index increment, which is close to $0.19\,\mathrm{ml\,g^{-1}}$ for all studied proteins (Zhao *et al.* 2011), and the refractive index of water at 485 nm (http://refractiveindex.info/):

$$n = 1.3356 + 0.19C_p \quad (6)$$

By combining the above equations and rearranging, we find w:

$$w = 1 - \frac{C_p}{d_p} = 6.02 - 3.76n = 0.993 - 3.76\Delta n \quad (7)$$

If a change in cell volume is due to water redistribution alone, the expected relative volume, refractive index and the integral phase changes would have a form:

$$(V_2/V_1)_w = \frac{1 - w_1}{1 - w_2} \quad (8a)$$

$$\left(\frac{\Delta n_2}{\Delta n_1}\right)_w = \frac{0.993 - w_2}{0.993 - w_1} \quad (8b)$$

$$\left(\frac{\Delta \varphi_2}{\Delta \varphi_1}\right)_w = \frac{(1 - w_1)(0.993 - w_2)}{(1 - w_2)(0.993 - w_1)} \quad (8c)$$

Volume change calculated from eqn (8a) can be compared to the measured value $(V_2/V_1)_m$; however, since there is no simple formula for the confidence interval for this ratio, the results should be interpreted cautiously. The other important parameter, the total dry mass of protein per cell, is calculated as

$$m_p = C_p V = \frac{\Delta n + 0.0014}{0.19} V \quad (9)$$

Statistical analysis

The data were analysed by a two-tailed Mann–Whitney U test using IBM SPSS Statistics 22 (IBM Corp., Armonk, NY, USA).

Results and Discussion

To demonstrate that the method can successfully measure intracellular water, the cells were exposed to hypotonic or hypertonic solutions; TTD and brightfield images were collected both before the solution change and 5 min afterwards. While the volume of cells in a hypotonic solution increased by the factor $V_2/V_1 = 1.50 \pm 0.05$ ($n = 8$), there was no accompanying change in the total cell protein ($m_{p2}/m_{p1} = 1.02 \pm 0.02$). The results of a similar experiment with hypertonic solution were $V_2/V_1 = 0.60 \pm 0.01$ ($n = 8$), and $m_{p2}/m_{p1} = 1.03 \pm 0.03$.

Incubation of HeLa cells with ionomycin caused the development of necrotic blebs due to localized water accumulation (Ramírez-Camacho *et al.* 2008). Accordingly, a refractive index map (Fig. 2) generated as described in the legend to Fig. 1 clearly shows an increased water content within the blebs compared to the rest of the cell. On average, ionomycin treatment for 20 min produced a 2.3% water gain (with large variability between cells) but no change in the cell protein (Table 1). Thus, the results of both the osmotic shock and necrotic swelling experiments were consistent with expectations, indicating that the TIE–TTD method yields reliable data.

We next turned to the analysis of apoptotic cells; data from several separate experiments are listed in Table 1. Apoptosis was induced with transcription inhibitor ActD or with protein kinase inhibitor staurosporine. Staurosporine causes splitting of cells into numerous fragments whose association with parent cells may not be obvious (Fig. 3). Because of that, cell volume measurements on such samples are unreliable: indeed, the loss of protein from MDBK cells was as high as 30%. The refractive index analysis shows an increase

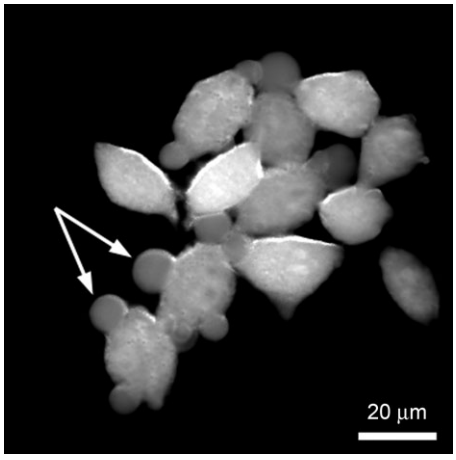

Figure 2. Qualitative refractive index map of ionomycin-treated HeLa cells
Necrotic blebs have a lower refractive index compared to the rest of the cell body, corresponding to elevated intracellular water.

© 2013 The Authors. The Journal of Physiology © 2013 The Physiological Society

Table 1. Results of apoptotic experiments

Cells	Treatment	Δn (10^{-3})	w	m_p (pg)	V (fl)	$(V_2/V_1)_m$
HeLa	Control	39.7 ± 3.4	0.844	517 ± 75	2503 ± 371	—
	Staurosporine	46.6 ± 5.3**	0.818	447 ± 124*	1735 ± 301**	—
	Ionomycin	33.6 ± 8.9*	0.867	527 ± 116	—	1.32 ± 0.29**
HeLa	Control	38.5 ± 1.9	0.848	362 ± 80	1953 ± 325	—
	ActD, deformed	65.1 ± 17.7**	0.748	301 ± 71*	973 ± 260**	—
HeLa	Control	39.8 ± 2.6	0.843	468 ± 99	2380 ± 640	—
	ActD, deformed	60.9 ± 15.7**	0.764	362 ± 119**	1229 ± 338**	—
MDBK	Control	33.0 ± 2.7	0.868	506 ± 132	—	—
	Staurosporine	37.1 ± 2.9**	0.854	362 ± 136**	—	—

The numbers are displayed as mean ± SD; statistical difference with untreated control is indicated by asterisks (*$P < 0.05$; **$P < 0.01$). Twenty cells were analysed for Δn measurements and approximately a hundred cells for the volume data. Only data for cells with abnormal morphology, indicating an advanced apoptotic stage, are presented for ActD-treated samples. Statistics on the volumes of MDBK cells was not obtained due to extensive cell clustering. The number in the last column shows the relative volume change measured on the same cells ($n = 20$) after 20 min of ionomycin treatment. Δn, difference between the refractive indices of the cell and of the medium; w, volume fraction occupied by intracellular water; m_p, total dry mass of protein per cell; V, cell volume; $(V_2/V_1)_m$, measured change in cell volume.

in n corresponding to a 1.5–2.5% decrease in intracellular water. This agrees with the common notion of the staurosporine action (Maeno *et al.* 2000; Ernest *et al.* 2008); at the same time, the measured decrease in w can account (in the case of HeLa cells) only for $V_2/V_1 = 0.86$ volume decrease compared to the measured factor of 0.69. This discrepancy suggests that the loss of apoptotic bodies may have contributed to the large decrease in the cell volume.

ActD treatment of HeLa cells starts producing detectable apoptotic changes after 8–10 h of incubation. An abrupt onset of blebbing nearly coincides with the loss of mitochondrial potential and is accompanied by temporary swelling (Kasim *et al.* 2013). A decrease in the cell volume develops several hours later; by the 14 h point used in this study many cells have already entered the shrinkage phase. Indeed, a significant water loss, from $w = 0.845$ down to 0.75–0.76, was observed in cells with apoptotic morphology (such as the group of cells in the central and upper part of Fig. 1). There was also about a 20% loss of cell protein, implying that cell volume measurements at this stage would produce an exaggerated picture of cell dehydration: $(V_2/V_1)_m = 0.50$ *vs.* $(V_2/V_1)_w = 0.60$–0.65.

The presented examples illustrate high sensitivity of the TIE–TTD method for studies of cell water regulation during pathological processes: indeed, the analysis of only small numbers of cells allows clear detection of water changes. Importantly, the analysis can be applied to samples where cell volume measurements alone would be inefficient; this can be due either to cell fragmentation or, conversely, due to aggregation of cells into tight clusters, where isolating individual cells for measurement can be difficult (such as with MDBK cells).

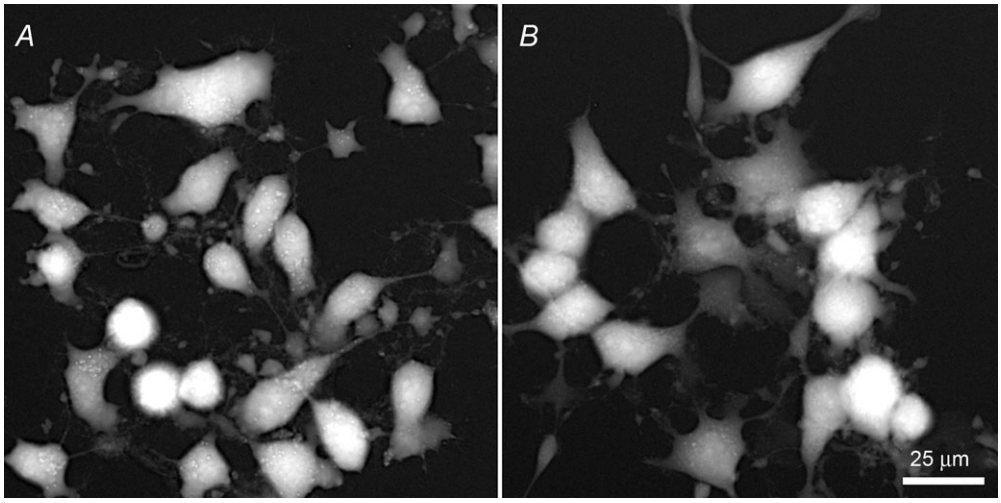

Figure 3. TTD images of HeLa (*A*) and MDBK (*B*) cells after exposure to staurosporine

© 2013 The Authors. The Journal of Physiology © 2013 The Physiological Society

One possible concern is the accuracy of eqn (5) and of the parameters used for the calculations. The combined contribution of lipids, nucleic acids and other non-protein types of molecules to the cell dry mass can be as high as 40% (Prescher & Bertozzi, 2005). However, their refractive index increment is expected to be similar to that of proteins (Wayne, 2009), and the results of calculations are tolerant to small errors. For example, if the assumed refractive index increment was $0.18\ \mathrm{ml\ g^{-1}}$ instead of $0.19\ \mathrm{ml\ g^{-1}}$, the calculated water content for $\Delta n = 0.05$ would only change from 0.805 to 0.7965.

TIE is not the only quantitative phase technique, and the same principle could be applied to others. There have been reports of application of digital holography to cell death (Pavillon *et al.* 2010, 2012; Khmaladze *et al.* 2012); however, in those studies the authors assumed constancy of the refractive index (see eqn (8b)) and ascribed all the observed phase changes to changes in the cell volume. Compared to digital holography, the attractiveness of TIE comes from its extreme technical simplicity and the ease of combining with volume measurements by TTD, so that the entire two-step process – phase and volume measurements – can be realized on a standard transmission microscope using a lamp for illumination. In the present realization, the main inconvenience, and possibly the main source of error, comes from uneven background in TIE-derived phase images. It might be possible to improve the quality of phase images by applying some of the more sophisticated TIE algorithms (Barbero & Thibos, 2006; Waller *et al.* 2010).

References

Antón JC, Alonso J, Pedrero JA & Quiroga JA (2012). Topographic optical profilometry by absorption in liquids. *Opt Express* **20**, 28631–28640.

Barbero S & Thibos LN (2006). Error analysis and correction in wavefront reconstruction from the transport-of-intensity equation. *Opt Eng* **45**, 94001.

Barty A, Nugent KA, Paganin D & Roberts A (1998). Quantitative optical phase microscopy. *Opt Lett* **23**, 817–819.

Chacon E, Reece JM, Nieminen AL, Zahrebelski G, Herman B & Lemasters JJ (1994). Distribution of electrical potential, pH, free Ca^{2+}, and volume inside cultured adult rabbit cardiac myocytes during chemical hypoxia: a multiparameter digitized confocal microscopic study. *Biophys J* **66**, 942–952.

Curl CL, Bellair CJ, Harris T, Allman BE, Harris PJ, Stewart AG, Roberts A, Nugent KA & Delbridge LM (2005). Refractive index measurement in viable cells using quantitative phase-amplitude microscopy and confocal microscopy. *Cytometry A* **65**, 88–92.

Ernest NJ, Habela CW & Sontheimer H (2008). Cytoplasmic condensation is both necessary and sufficient to induce apoptotic cell death. *J Cell Sci* **121**, 290–297.

Fischer H, Polikarpov I & Craievich AF (2004). Average protein density is a molecular-weight-dependent function. *Protein Sci* **13**, 2825–2828.

Gómez-Angelats M & Cidlowski JA (2002). Cell volume control and signal transduction in apoptosis. *Toxicol Pathol* **30**, 541–551.

Gorthi SS & Schonbrun E (2012). Phase imaging flow cytometry using a focus-stack collecting microscope. *Opt Lett* **37**, 707–709.

Gu JJ, Yu YF, Li EP, Ng SH, Yap PH, Zhou XQ, Cheng TH & Liu AQ (2008). Real-time measurement of cellular refractive index and thickness using cell culture chip. In *12th International Conference on Miniaturized Systems for Chemistry and Life Sciences*. San Diego, CA, USA.

Hessler JA, Budor A, Putchakayala K, Mecke A, Rieger D, Banaszak Holl MM, Orr BG, Bielinska A, Beals J & Baker J Jr (2005). Atomic force microscopy study of early morphological changes during apoptosis. *Langmuir* **21**, 9280–9286.

Kasim NR, Kuželová K, Holoubek A & Model MA (2013). Live fluorescence and transmission-through-dye microscopic study of actinomycin D-induced apoptosis and apoptotic volume decrease. *Apoptosis* **18**, 521–532.

Kerr JF, Wyllie AH & Currie AR (1972). Apoptosis: a basic biological phenomenon with wide-ranging implications in tissue kinetics. *Br J Cancer* **26**, 239–257.

Khmaladze A, Matz RL, Epstein T, Jasensky J, Banaszak Holl MM & Chen Z (2012). Cell volume changes during apoptosis monitored in real time using digital holographic microscopy. *J Struct Biol* **178**, 270–278.

Lue N, Popescu G, Ikeda T, Dasari RR, Badizadegan K & Feld MS (2006). Live cell refractometry using microfluidic devices. *Opt Lett* **31**, 2759–2761.

Maeno E, Ishizaki Y, Kanaseki T, Hazama A & Okada Y (2000). Normotonic cell shrinkage because of disordered volume regulation is an early prerequisite to apoptosis. *Proc Natl Acad Sci U S A* **97**, 9487–9492.

Model MA (2012). Imaging the cell's third dimension. *Microsc Today* **20**, 32–37.

Model MA, Khitrin AK & Blank JL (2008). Measurement of the absorption of concentrated dyes and their use for quantitative imaging of surface topography. *J Microsc* **231**, 156–167.

Orlov SN, Platonova AA, Hamet P & Grygorczyk R (2013). Cell volume and monovalent ion transporters: their role in triggering and progression of the cell death machinery. *Am J Physiol Cell Physiol* **305**, C361–C372.

Pavillon N, Benke A, Boss D, Moratal C, Kühn J, Jourdain P, Depeursinge C, Magistretti PJ & Marquet P (2010). Cell morphology and intracellular ionic homeostasis explored with a multimodal approach combining epifluorescence and digital holographic microscopy. *J Biophotonics* **3**, 432–436.

Pavillon N, Kühn J, Moratal C, Jourdain P, Depeursinge C, Magistretti PJ & Marquet P (2012). Early cell death detection with digital holographic microscopy. *PLoS One* **7**, e30912.

Platonova A, Koltsova S, Maksimov GV, Grygorczyk R & Orlov SN (2011). The death of ouabain-treated renal epithelial C11-MDCK cells is not mediated by swelling-induced plasma membrane rupture. *J Membr Biol* **241**, 145–154.

Prescher JA & Bertozzi CR (2005). Chemistry in living systems. *Nat Chem Biol* **1**, 13–21.

Ramírez-Camacho R, García-Berrocal JR, Trinidad A, Verdaguer JM & Nevado J (2008). Blebs in inner and outer hair cells: a pathophysiological hypothesis. *J Laryngol Otol* **122**, 1151–1155.

© 2013 The Authors. The Journal of Physiology © 2013 The Physiological Society

Schonbrun E, Di Caprio G & Schaak D (2013). Dye exclusion microfluidic microscopy. *Opt Express* **21**, 8793–8798.

Tychinsky VP & Tikhonov AN (2010). Interference microscopy in cell biophysics. 1. Principles and methodological aspects of coherent phase microscopy. *Cell Biochem Biophys* **58**, 107–116.

Waller L, Tian L & Barbastathis G (2010). Transport of intensity phase-amplitude imaging with higher order intensity derivatives. *Opt Express* **18**, 12552–12261.

Wayne RO (2009). *Light and Video Microscopy*. Academic Press, Burlington, MA, USA.

Zhao H, Brown PH & Schuck P (2011). On the distribution of protein refractive index increments. *Biophys J* **100**, 2309–2317.

Additional information

Competing interests

The authors declare no competing interests.

Author contributions

M.A.M. designed and performed the experiments, analysed the data and wrote the manuscript. E.S. developed the program for solving the TIE equation and contributed to preparation of the manuscript. Both authors approved the final version of the manuscript. Experiments were carried out at Kent State University.

Funding

This work was partly funded by NIH grant 1R15GM186816 to M.A.M.

Acknowledgements

We thank Dr Douglas Kline for the gift of the MDBK cell line and Sarah Samblanet for help with statistical analysis.

© 2013 The Authors. The Journal of Physiology © 2013 The Physiological Society